metals

MDPI

Article

A Determination of the Influence of Technological Parameters on the Quality of the Created Layer in the Process of Cataphoretic Coating

Jozef Dobránsky [1,*], Miroslav Gombár [2], Patrik Fejko [1] and Róbert Balint Bali [1]

[1] Faculty of Manufacturing Technologies with a Seat in Presov, Technical University of Kosice, Sturova 31, 080 01 Presov, Slovakia; patrik.fejko@tuke.sk (P.F.); robert.balint.bali@tuke.sk (R.B.B.)
[2] Faculty of Management and Business, University of Presov, Namestie Legionarov 3, 080 01 Presov, Slovakia; miroslav.gombar@unipo.sk
* Correspondence: jozef.dobransky@tuke.sk; Tel.: +421-55-602-6350

Abstract: Cataphoresis varnishing enables an organic coating to form on an aluminum substrate, thus increasing its corrosion resistance and durability. Cataphoresis varnishing is known to ensure a high adhesion of the created cataphoresis layer and a good homogeneity of this layer, even on surfaces with complex geometry. This paper aimed to optimize the deposition process and to analyze and evaluate the thickness of a cataphoresis layer formed on an aluminum substrate from AW 1050—H24 material. In total, 30 separate samples were created in accordance with the Design of Experiments methodology, using a central composite plan. The independent input factors in the study were: the electrical voltage (U) and deposition time in the cataphoresis varnishing process (t_{KTL}) at the polymerization times of 15 min, 20 min, and 25 min, respectively. The results of the statistical analysis showed that the voltage accounted for 33.82% of the change in the thickness of the created layer and the deposition time contributed 28.67% to thi change. At the same time, the interaction of the voltage and deposition time ($p < 0.0001$) accounted for 20.25% of the change in the thickness of the layer under formation. The regression model that was constructed showed a high degree of prediction accuracy (85.8775%) and its use as a function for nonlinear optimization provided a maximum layer thickness t_h of max = 26.114 µm, at U = 240 V and t_{KTL} = 6.0 min, as was proven under experimental conditions.

Keywords: cataphoresis; electrophoresis; coating layer thickness; analysis; planning conditions

check for updates

Citation: Dobránsky, J.; Gombár, M.; Fejko, P.; Balint Bali, R. A Determination of the Influence of Technological Parameters on the Quality of the Created Layer in the Process of Cataphoretic Coating. *Metals* **2023**, *13*, 1080. https://doi.org/10.3390/met13061080

Academic Editor: Wangping Wu

Received: 20 April 2023
Revised: 3 June 2023
Accepted: 5 June 2023
Published: 7 June 2023

1. Introduction

Electrophoretic paints, commonly known as electrocoats or paints, are organic coatings dispersed in water that carry an electric charge. This enables the paint to be used for deposition onto a metal that is carrying an opposite charge. Special needs for formulating this coating result from this special way of application [1–3].

Automotive coatings and the processes used to paint automotive surfaces exemplify avant-garde technologies capable of producing durable surfaces that exceed customer expectations for appearance, maximizing efficiency, and meeting environmental regulations. These achievements are rooted in 100 years of experience, trial and error techniques, technological advances, and theoretical evaluation [4].

The overall critical performance factors that drive the development and use of advanced automotive coatings and coatings technology are aesthetic properties, corrosion protection, mass production, cost, environmental requirements, appearance, and durability [5].

The adhesion of the coating to the material is also a very important factor for the appearance and durability of the surface of the material. Based on research, a torsional delamination test was developed, which consisted of applying an increasing torque on a

hexagonal base directly glued to the coating. The test was quantitative and made it possible to calculate the shear stress that arose during delamination. Based on this test, it was found that polymerization temperature is an important factor in the adhesion of the material [6].

Anti-corrosion protection is also provided to ensure the durability of the coating. One of the technologies used to ensure this anti-corrosion protection is cataphoresis, which is used to apply paint to the paint surface. It is known for ensuring a high coating adhesion and good homogeneity, even for surfaces with complex geometry [7–9].

The researchers Mr. Rossi, Calovi, and Fedel conducted research for the implementation and optimization of the deposition process and the evaluation of the properties of a cataphoretic coating applied to an aluminum foam. They found a large effect for the corrosion behavior of the painted foam, which was evaluated using acetic acid salt chamber exposure and electrochemical impedance spectroscopy. By inserting the dye into the resin, it was possible to observe three types of cells, namely, black-colored cells that represented the coating; light-colored cells without traces of the coating resin; and cells with a purple color, which represented traces of resin. It was found that it is very difficult to obtain a uniform coating on the entire surface of aluminum according to the foam sample; another important factor is the deposition voltage, which achieves coatings with a greater thickness [10].

In further research, it was also confirmed that the higher the coating voltage, the greater the thickness of the layer. However, the cataphoresis process appears to be a promising technique for coating a material surface. If we set a relatively smaller coating voltage, it is possible to obtain a relatively thin coating, while it is necessary to avoid exceeding the coating voltage to values that are too high, which can lead to the formation of bubbles [11–13].

Other methods of applying organic coatings include adding graphene oxide to a cataphoresis bath. Research has found that graphene oxide leads to the formation of defective layers, with the consequence of reducing the durability of the coating. However, when applied in two steps with two different baths, it is possible to maintain the integrity of the coating and ensure the protection of the substrate. In the first bath, an epoxy-based method has been used, where an epoxy resin was used, which ensured an excellent level of material adhesion and good mechanical properties of the coating. The second bath contained graphene oxide, also called the black bath. From this research, we can determine only one thing: that the black bath guarantees a much greater thickness of the layer, thereby guaranteeing excellent protection [14–17].

In further research, the authors looked at the compatibility between the cataphoretic electrocoating and a silane surface layer. The research was carried out on a sheet of steel that had previously been treated with a silane sol-gel. In the case of thin samples coated with 120 nm silane sol-gels, the electrodeposition conditions were slightly affected. On the contrary, at a greater thickness, degradation occurred due to hydrogen production and bubbling [18–20].

The authors see the present paper as a contribution to the procedural approach to the complex process of creating anti-corrosion layers, such as the process of cataphoresis varnishing. Since the technological processes of surface treatment represent multifactor systems with interacting physical, chemical, and technological effects and, at the same time, since their influences may be considered random variables, the authors subjected the experimentally obtained data to proper methods of statistical analysis to gain a deeper understanding of these interrelationships. Another undisputed benefit of the present paper is the nonlinear optimization (maximization) of the basic technological parameter, the thickness of the created layer, and the analysis of the rate of deposition in the process of cataphoresis varnishing. However, the limitations are those of the experiment constraints and the use of only two basic process factors.

2. Materials and Methods

With the need to minimize costs and time and, at the same time, to maximize the reliability and objectivity of the information obtained about the process of anodic aluminum oxidation, it was necessary to conduct the experiment with as few trials as possible. The experimental planning methodology—DoE (Design of Experiments)—was used for the experimental verification of the influence of the basic process factors on the thickness of the layer created by the cataphoresis. This methodology represented the only scientifically justifiable methodology of experimentation and allowed for an obtainment of the maximum amount of information with a high statistical and numerical correctness, i.e., with a high reliability of the implemented conclusions and an optimal (minimum) number of individual trials. For the purpose of the experimental verification of the influence of the selected process factors (deposition time, varnishing voltage, and polymerization time), a Central Composite Plan was chosen, which facilitated the creation of a non-linear model, which we assume, in view of our practical experience, to be the case. The total number of trials, in terms of the type of the plan used, was 10. Since the marginal intention was also to examine the influence of the polymerization time (t_{pol} = 15 min, 20 min, and 25 min) at a constant polymerization temperature (T_{pol} = 200 °C) on the thickness and adhesion of the cataphoresis varnish, the experiment was carried out in three separate blocks. Each block represented one polymerization time [21,22].

The basic knowledge of the technological process and the method of its management could be obtained through the method of a factor experiment. The result of the factor experiment was an interpolation model that had the form of a first- or higher-degree polynomial (linear or non-linear model). In the analysis, we obtained results that allowed us to discover stages of the technological process. The planning of the technological process for the linear model can be written with the mathematical equation:

$$\hat{y} = b_0 + \sum_{j=1}^{k} b_j \cdot x_j \quad (1)$$

Surface areas with higher-order models can be described more accurately if it is not possible to create an adequate linear model. We can write the technological process planning for the non-linear model using the mathematical equation:

$$\hat{y} = b_0 + \sum_{j=1}^{k} b_j \cdot x_j + \sum_{j \neq g=1}^{k} b_{jg} \cdot x_j \cdot x_g + \sum_{j=1}^{k} b_{jj} \cdot x_{jj}^2 \quad (2)$$

Within relations (1) and (2), $\hat{y}$ represents the estimate of the investigated parameter (the thickness of the created layer), x_i represents the independent variables (U_{KTL}, t_{KTL}, and t_{pol}), and b_0, b_i, b_j, b_{jg}, and b_{jj} represent the estimates of the regression coefficients, which were calculated based on the method of least squares.

To reduce the number of experiments and utilize the results of the linear model experiment, we used composition plans. According to the location of the points, we divided composition plans into central and non-central [23].

2.1. Material Selection

In the elaboration of the work, namely, the analysis of the effect of the cataphoresis coating process conditions on the layer quality of the aluminum parts, aluminum specimens of the AW–1050 H24 type were used. Today, aluminum is used to produce various types of components for the automotive industry. EN AW–1050 A is a non-alloy aluminum with a maximum impurity content of 0.5%. The material is thermally uncurable. Increasing its strength is possible only under cold conditions (by rolling and pulling, etc.), when the increase in this strength is related to a reduction in elasticity and, thus, formability. In the soft annealed state (0), the material has an excellent formability (by bending and deep drawing, etc.). In the hardened states of H14 and H24, this formability is substantially lower. It should be taken into account that the H24 state exhibits a slightly better formability than that of the H14 state. It is used, among others, in the production of storage tanks, heat

exchangers, spotlights, and packaging materials, etc. Its corrosion resistance is excellent under normal atmospheric conditions. This can be improved by the products' technical anodic oxidation. Non-alloy aluminum is very weldable using all common aluminum welding procedures (especially the MIG and TIG gas arc welding procedures). Under certain conditions, it may be necessary to soft anneal the material. This soft annealing temperature is from 320 to 350 °C [24–26].

2.2. Technological Process of Production

The experiment was carried out as part of a production operation on an automated cataphoresis line. The preparation of each sample, before the actual cataphoresis coating, was as follows:

(a) Chemical degreasing of the samples—chemical degreasing was carried out in a high alkaline medium emulsifying agent containing low-foaming tensides. Each sample was subjected to a degreasing time of 8 min under a constant temperature of 65 °C with a constant chemical composition of the solution (40 g·L^{-1}). The degreasing was followed by a two-stage rinse in demineralized water.

(b) Pre-phosphating activation—this was carried out in a commercial preparation from Pragochema CZ, trade name Pragofos 1927, under the following constant conditions: pH = 9.5, T_{act} = 40 °C, and t_{act} = 2 min.

(c) Phosphating—the phosphating itself was carried out in a multi-cation phosphatizing solution without nitrite accelerators. The samples were phosphated under constant operating conditions: T_{ph} = 50 °C and t_{ph} = 5 min and a constant chemical composition: a total Fisher spot content of 16 points, a free acid content of 0.8 g·L^{-1}, an accelerator content of 2.3 g·L^{-1}, a zinc content of 0.95 g·L^{-1}, and a phosphate content of 12.5 g·L^{-1}, with a pH of 3.40. The surface weight of the deposited phosphate coating ranged from 1.97 to 2.09 g·m^{-2}. The surface homogeneity after phosphating can be seen in the image of the checking sample shown in Figure 1. The SEM images were captured using a Scanning Electron Microscope Tescan Mira 3 FE equipped with an integrated EDX analyzer from Oxford Instruments, which allowed for an observation of the microstructure of the material and the performance of an elemental analysis (spot and surface distribution). For the SEM images, the secondary electron mode (SE) and an accelerating voltage of 15 kV were used. The distance between the sample and detector was 15 mm and the view field was 185 µm. A three-stage rinse in demineralized water followed the phosphating process.

(d) Cataphoresis varnishing—this was carried out according to the matrix of the experiment plan using a central composite plan. The basic variable factors are presented in Table 1. In the cataphoresis varnishing of the individual samples, the constant temperature of the cataphoresis paint was T_{KTL} = 32.5 °C and the value of the current flowing through the electrochemical system, namely I_{KTL} = 200 A, was kept constant. The chemical parameters of the cataphoresis paint during the experiment were also maintained at a constant level: dry matter (1 h at 110 °C) at 15.300, P/B ratio (binder/paint) at 0.151, pH (at 25 °C) at 5.82, and conductivity (at 25 °C) at 1660 µS·cm^{-1}.

Table 1. Values of variable input factors.

Factor Code	Factor	Unit	Factor Level				
			−2	**−1**	**0**	**+1**	**+2**
x_1	U_{KTL}	V	200	220	240	260	280
x_2	t_{KTL}	min	3.0	4.5	6.0	7.5	9.0
x_3	t_{pol}	min		15	20	25	

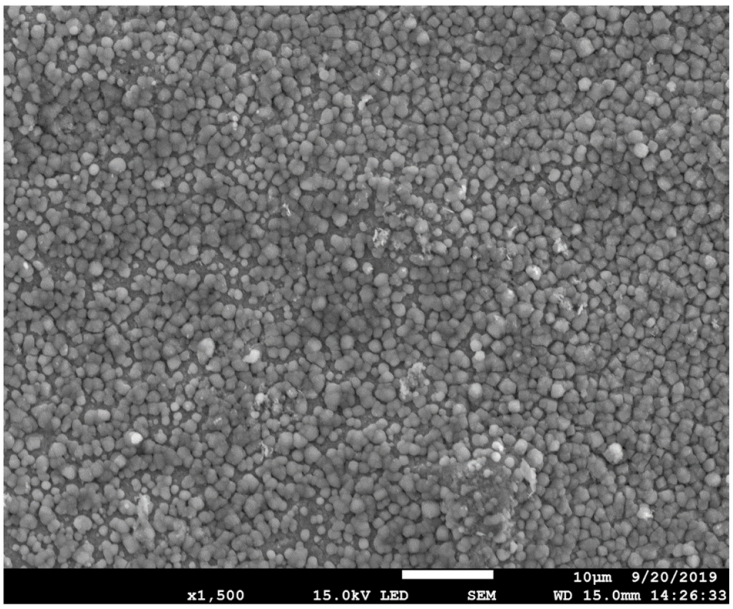

Figure 1. Homogeneity of the phosphate layer during the experiment (m_S = 1.97 g·m^{-2}).

In the actual implementation of the experiment, the Design of Experiments methodology was used, including the selection of the central composite plan. Table 1 shows the basic levels of the experiment plan for the individual input factors where, through their combination, individual experiments were carried out. The particular levels of the input factors were selected based on the practical experience of the authors.

2.3. Thickness Measurement

The layer thicknesses on the individual aluminum specimens were measured with the Elcometer 456 digital thickness gauge. This apparatus autonomously evaluated the average value of the coating when measured at specified points. The coating thickness ranged from 15 µm to 70 µm on the individual specimens. The measurement itself produced three types of measurement errors, i.e., systematic measurement errors, which were detected from the statistics, random errors (could not be influenced, they occurred during the measurement and were caused either by a failure to clean the surface of the components or by the influence of the temperature fluctuations, etc.), and gross errors (caused by observer fatigue and inattention) [27].

3. Results and Discussion

The process of cataphoresis varnishing can be viewed from two angles. The first is the electro-osmotic theory of cataphoresis. It is assumed that an electric bi-layer emerges at the interface between the solid and liquid phase. A part of this double layer is deposited as a liquid coating on top of the solid phase and the other part is scattered in the adherent liquid layer. As long as the solid phase can move freely in the liquid, the tangential component of the electrical force sets the suspended particles into motion. Cataphoresis varnishing uses the principle of cathodic organic coating creation based on epoxy or acrylic cataphoresis materials. Water-soluble cationic coatings with very low organic solvent content contain particles of varnish in the form of polymer cations. Thus, if an electric field is created in this system, with the solid phase particles scattered in the liquid phase, the particles begin to move in the direction of the electric field under the influence of the electric force. A direct current between the coated part, which is the cathode in the cataphoresis varnishing process, and an anodic counter electrode (anode) creates an electric field that becomes the carrier of the polymer cations that travel towards the cathode. In the course of the reactions with hydroxyl ions resulting from the breakdown of water, the solubility is suppressed on the cathode, and the organic coating deposition process is activated on the surface of

the cathode. The second view of the cataphoresis varnishing process is the ionic theory of cataphoresis. In this theory, suspended particles are considered to be high-molecular-weight electrolyte molecules. These molecules then disassociate into high-power ions and associated electrolytic ions, which carry the same amount of electrical charge, but of the opposite polarity. The moving particles of the solid phase, which are suspended in the liquid phase under the influence of the electric field, are seen as electrolytic ions in electrolyte solutions. The electric charges of the ions are affected by an electric force in the electric field, the magnitude of which is determined by the product of the magnitude of the electric charge and the magnitude of the electric field. This force accelerates the ion, which is, at the same time, hampered by the movement of the frictional force emerging in the liquid environment. The ion is, at this time, considered to be a sphere with a radius corresponding to its resistance in the given environment, defined by the Stokes equation of resistance of a sphere in a liquid. The friction force is proportional to the velocity of the ion. Upon the introduction of the electrical charge, a steady state occurs. The mobility of the ions is directly proportional to the power and inversely proportional to the radius of the ion [28,29].

Since the implemented methodology of the experimental verification (Design of Experiments) represented a statistical approach, the subsequent analysis of the experimentally obtained data was, too, carried out using mathematical–statistical procedures. The initial analysis of the applied model pointed to the fact that the proportion of the variability of the measured thickness of the cataphoresis coating was 86.70225% and the adjusted index of determination, determining the degree of explanation of the data variability by the model, was 85.8775%. The average thickness of the cataphoresis layer formed, covering all the individual trial runs, was $t_h = 24.464 \pm 3.677$ μm.

The table of the variance analysis (Table 2), as a basic requirement for the correctness of the regression model, enabled us to conclude that the variability caused by random errors was significantly lower than the variability of the measured values explained by the model, and the value of the achieved significance level (p) indicated the adequacy of the model used, based on the Fisher–Snedecor test criterion. Another view of this analysis is through assessing the adequacy of the model itself and is based on the very essence of the variance analysis. For testing the null (H_0) statistical hypothesis, which followed from the nature of the test and said that none of the effects (factors) used in the model effected a significant change on the examined variable, it followed that the achieved level of significance (p) was less than the selected level of significance $\alpha = 0.05$, and it could be concluded that we did not have enough evidence to accept H_0 and we could say that the model was significant [30].

Table 2. The table of variance analysis.

Source	df	SS	MS	F	*p*
Model	5	3956.890	791.378	58.5323	<0.0001 *
Error	144	1946.932	13.52		
C. Total	149	5903.821			

SS—Sum of Squares, MS—Mean squares, F—Fisher's test statistic, p—achieved level of significance, and *—significant at the level of significance $\alpha = 0.05$.

The applied model was further tested in the so-called insufficient model adaptation error test (Table 3), where we tested the scatter of the residues and scatter of the data measured within the groups; thus, we tested the premise of whether the regression model adequately described the observed dependence. Based on the error test of insufficient model adaptation, due to the achieved significance level of 0.1853, a zero statistical hypothesis could be accepted at the selected significance level of $\alpha = 5\%$ and it could be said that the scatter of the residues was less than or equal to the scatter within the groups and, therefore, the model could be considered sufficient.

Table 3. Model fit error.

Source	df	SS	MS	F	*p*
Lack Of Fit	3	283.9322	94.6441	8.0245	0.1853
Pure Error	141	1663.000	11.7943		
Total Error	144	1946.932			

SS—Sum of squares, MS—Mean square, F—Fisher's test statistic, and *p*—achieved level of significance.

Based on the above assumptions and their fulfillment (Tables 2 and 3), the following table (Table 4) presents an estimate of the regression model parameters with testing the significance of the individual effects and their combination at the significance level $\alpha = 0.05$.

Table 4. Estimates of regression model coefficients.

Term	Estimate	Std Error	t	*p*	−95% CI	+95% CI
Intercept	26.114	0.567	46.030	<0.0001 *	24.993	27.236
x_1	3.170	0.274	11.560	<0.0001 *	2.628	3.711
x_2	2.686	0.274	9.800	<0.0001 *	2.144	3.227
$x_1 \cdot x_2$	3.286	0.475	6.920	<0.0001 *	2.347	4.224
$x_1 \cdot x_1$	−0.474	0.233	−2.030	0.0439 *	−0.934	−0.013
$x_2 \cdot x_2$	−0.902	0.233	−3.870	0.0002 *	−1.362	−0.441

x_1—voltage (V), x_2—deposition time (min), t—Student's test criterion, *p*—achieved level of significance, CI—confidence interval, and *—significant at the level of significance $\alpha = 0.05$.

The results shown in Table 4 thus enabled the building of a predictive mathematical-statistical model at a coded scale:

$$y(t_h) = 26.114 + 3.170 \cdot x_1 + 2.686 \cdot x_2 + 3.286 \cdot x_1 \cdot x_2 - 0.474 \cdot x_1^2 - 0.902 \cdot x_2^2 \quad (3)$$

Since the DoE methodology worked with a code scale, in order to ensure the numerical and statistical correctness of the results, it was necessary to convert Equation (3) to the scale of the original variables, the natural scale. Considering that the code scale represented the DoE standardization of the variable input factors, it was necessary to use the following equation to convert to the natural scale:

$$X_d(i) = \frac{x(i) - \frac{x_{max} + x_{min}}{2}}{\frac{x_{max} - x_{min}}{2}} \quad (4)$$

where $x(i)$ represents the original basic variable, $i = 1, 2, \ldots, n$ is the number of basic factors, x_{max} is the maximum value of the original variable $x(i)$, and x_{min} is the minimum value of the original variable $x(i)$.

Thus, when using the regression model (3) in the code scale, taking into account the conversion Equation (4) for the individual variable input factors and subsequent adjustment, it was possible to make a notation of a prediction equation for the thickness of the cataphoresis layer in the form of:

$$th = 52.370 + 7.01 \cdot 10^{-2} \cdot U - 19.687 \cdot t_{KTL} + 0.109 \cdot U \cdot t_{KTL} - 1.185 \cdot 10^{-3} \cdot U^2 - 0.409 \cdot t_{KTL}^2 \quad (5)$$

The analysis of Table 4 showed that the largest share in explaining the variability in the parameter under study, the thickness of the cataphoresis layer per absolute element of the model (intercept), which was involved in changing the thickness value of the layer, was that of 57.387%. From a methodological point of view, the absolute element of the model was characterized by "neglected" influences, which we kept at a constant level in the experiment (especially the chemical characteristics of the cataphoresis electrolyte, current density, and anode-to-cathode ratio), or we did not consider them. If we neglected this model element and subsequently analyzed only the basic variable input factors, we would have come to

the conclusion (Table 4) that the most significant factor that affected the thickness of the layer formed was the voltage (U). It accounted for 33.82% of the change in the thickness of the layer. The second most significant element of the model (5) was the deposition time in the cataphoresis varnishing process (t_{KTL}), accounting for 28.67% of the change in the thickness. At the same time, the interaction of the voltage and deposition time accounted for 20.25% of the change in the thickness of the layer formed. The nonlinear model elements (5), namely, the voltage squared and the deposition time squared, accounted for 5.94% and 11.32%, respectively, of the change in the thickness of the created layer. As seen in Table 4 and model (5), it was clear that the processes of the surface treatment of the metals, including the cataphoresis varnishing, were best described by non-linear models with a significant influence and mutual interaction of the individual factors. The model (5) also needed to be expanded and modified by the influence of the chemical factors acting in the process of the cataphoresis varnishing. The model (5) represented a steppingstone to a comprehensive analysis of the cataphoresis varnishing process using a statistical approach. The statistical approach was chosen because the studied layer parameters were understood as random variables in the mathematical sense [31].

The plotted thickness of the cataphoresis layer formed during the respective deposition times in the cataphoresis coating process under various voltages is shown in Figure 2.

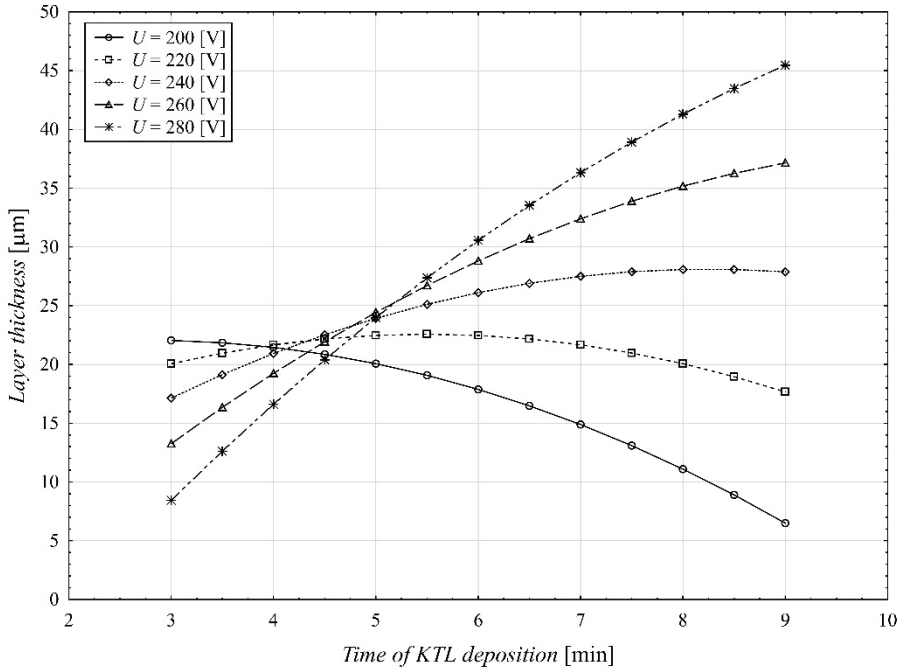

Figure 2. Dependence of the thickness of the formed layer on the time of KTL deposition at different voltage values.

The graph shows that, by increasing the deposition time of the varnishing medium, the thickness of the layer formed was reduced under different varnishing voltages. A varnishing voltage of 200 V and a deposition time of the varnishing medium of 3 min affected the layer thickness the most. The thickness of the layer increased during the 3 min deposition period, after which, the thickness of the layer decreased. This was due to a low electric current, which caused the coagulation of the paint on the surface where it stopped; thus, the coated part became electrically non-conductive. With an increased varnishing medium deposition time, the value of the electric current decreased due to an increase in the thickness of the deposited layer t_h, and the value of the current decreased to zero.

Under a 220 V voltage, the thickness of the coating increased for 5.5 min when the coating also reached its maximum thickness. After this time, the thickness of the coating decreased. Increasing the varnishing voltage to 240 V meant increasing the deposition

time of the varnishing medium up to 8 min, without significantly affecting the thickness of the layer. A further increase in the varnishing voltage resulted in an accelerated layer formation and a similar change was observed when the varnishing voltage was increased to 260 V and 280 V, when the thickness of the layer reached its maximum values throughout the deposition time of the varnishing medium t in the electrolyte. This phenomenon could be attributed to the color deposition technology that ran in the following sequence: water electrolysis, ion migration (electrophoresis), the coagulation of the polymer on the cathode, and water ejection via osmotic pressure. This phenomenon, as such, could be explained by Ohm's law, which says an electric current of a constant voltage is created between a cathode and anode, which can be described by the equation U = R*I. Cataphoresis varnishing works on the principle of creating cathodic organic coatings based on epoxy materials. Cationic coatings soluble in water contain a small number of organic solvents and, at the same time, particles in the form of polymer cations.

Once the coating was deposited on the cathode in the process of cataphoresis, the resistance reached its maximum values. The layer ceased to be conductive and became insoluble in water again. This deposited layer needed to be subsequently cured in a reaction with another polymer. At this stage, hydroxyl groups along the molecular chain in the cationic resin were applied, which reacted with isocyanates (they were equally present in the resin) to form urethane compounds.

The function gradient (5), i.e., the direction of the steepest addition to the layer thickness under the input parameters examined, namely the voltage (U) and the deposition time in the course of the cataphoresis varnishing (t_{KTL}), is defined by the vector:

$$\nabla t_h(U, t_{KTL}) = [0.10953 \cdot U - 0.80176 \cdot t_{KTL} - 19.6867; 0.10953 \cdot U - 0.0037 \cdot t_{KTL} + 0.0701] \quad (6)$$

The relationship (6) thus defines the direction, depending on the input variables, in which the function (5) grew the fastest, that is, the direction where the thickness of the forming layer reached its maximum in the shortest possible time.

In terms of the cataphoresis layer formation, based on the mathematical–statistical models (5) and (6), it is possible to define the layer formation rate as the first derivative of the function (5), according to the deposition time (t_{KTL}):

$$v_{th} = \frac{\partial t_h}{\partial t_{KTL}} = 0.10953 \cdot U - 0.80176 \cdot t_{KTL} - 19.6867 \quad (7)$$

Thus, Equation (7) represents the direction of the steepest rise in the function (6) in the direction of the voltage. Thus, from Equation (7), it follows that the rate of formation of the cataphoresis layer under the given experimental verification conditions (Table 1) was a function of the voltage and deposition time in the process of the cataphoresis varnishing. In accordance with theoretical knowledge and on the basis of Equation (7), we can conclude that, by increasing the voltage, the rate of deposition of the cataphoresis layer also increased, and, on the other hand, by increasing the deposition time, this rate in the cataphoresis varnishing process decreased. The decrease in the rate of the formation of the cataphoresis layer and the influence of the deposition time depended on the electrical properties of the forming layer. Considering the fact that the layer formed during cataphoresis was electrically non-conductive, its electrical resistance must have inevitably increased with an increase in its thickness; therefore, the rate of its formation must have decreased. However, if we wanted to ensure a constant rate of formation of the layer throughout the entire deposition period in the cataphoresis varnishing process, we would have to increase the voltage in proportion, as per Equation (7). The rate of the formation of the layer is a fairly important indicator of the cataphoresis varnishing process. However, there are two opposing requirements of the rate of the layer formation. On the one hand, there is a requirement to achieve the highest possible rate of layer formation, thereby reducing the time required for the cataphoresis varnishing to run its course, which results in an increased economic efficiency of the process itself. The counter requirement stems from the process

of layer formation in relation to its quality. If the rate of the layer formation is too high, the hydrogen that emerges on the surface of the treated structural part does not have enough time to "escape" the surface, and the resulting layer "traps" it in the surface of the part. However, in the process of polymerization, this trapped hydrogen creates defects in the layer in the form of craters. Further research is needed to determine the optimal value for the rate of deposition, taking into account the basic requirements above [32].

Equation (7) is a statistical equation and, therefore, within, it holds only the input variables' intervals and the factors used (Table 1). Its extrapolation beyond these factor values intervals may lead to incorrect results and conclusions.

The second partial part of the analysis, shown in Table 1, was devoted to the evaluation of the thickness of the cataphoresis layer in relation to the polymerization time (t_{pol}), using three different times as part of the experiment plan, namely 15 min, 20 min, and 25 min, respectively, for each combination. The basic graphical representation of the influence of the polymerization time on the thickness of the layer created in individual combinations of the input factors (U, t_{KTL}) is shown in Figure 3.

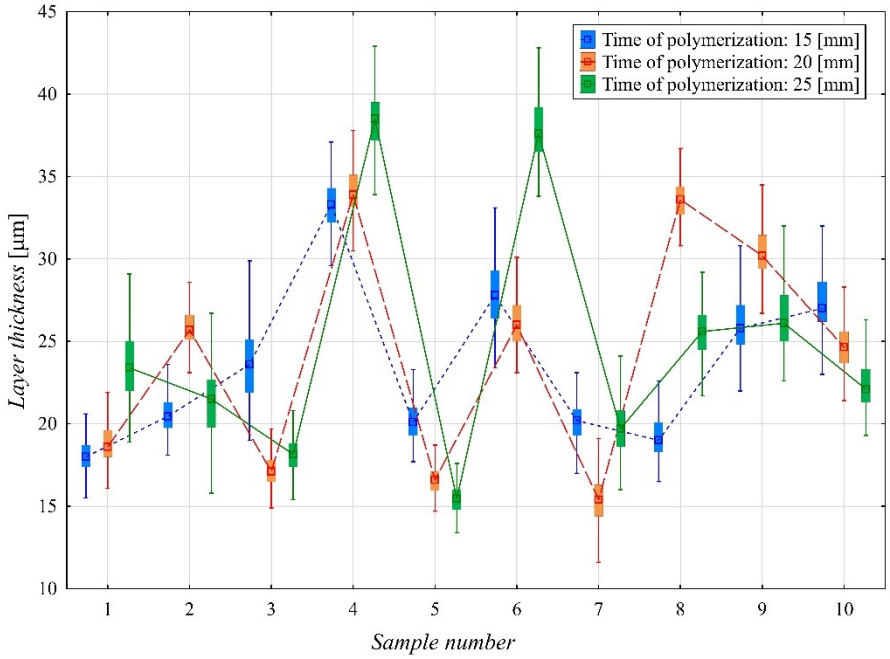

Figure 3. Effect of polymerization time on the thickness of the cataphoretic layer for individual experiments.

Figure 3 makes it evident that the polymerization time affected the resulting thickness of the cataphoresis layer in a relatively random manner. However, the polymerization process itself showed that, depending on the type of cataphoresis paint used, 10% and 20% of it was lost in the polymerization process. This was because the polymerization process did not directly participate in the formation of the cataphoresis layer, but affected its resulting properties. The average thickness of the cataphoresis layer formed after the polymerization at a constant temperature of 200 °C and a polymerization time of 15 min was 23.709 ± 0.192 µm. Here, it is necessary to say that in this analysis, all the values of the measured thickness were used, including repetitions of individual measurements (7565 measurements). For a polymerization time of 20 min at a constant temperature of 200 °C, the average thickness value of the formed layer was 24.349 ± 0.267 µm, and for a polymerization time of 25 min, the average thickness of the layer was 24.937 ± 0.289 µm.

Thus, the average difference in the thickness of the cataphoresis layer between the individual polymerization times was 0.613 ± 0.103 µm between the polymerization times of 20 min and 15 min, 0.619 ± 0.102 µm between the polymerization times of 25 min and 20

min, and finally, 1.220 ± 0.102 µm between the polymerization times of 25 min and 15 min (Figure 4).

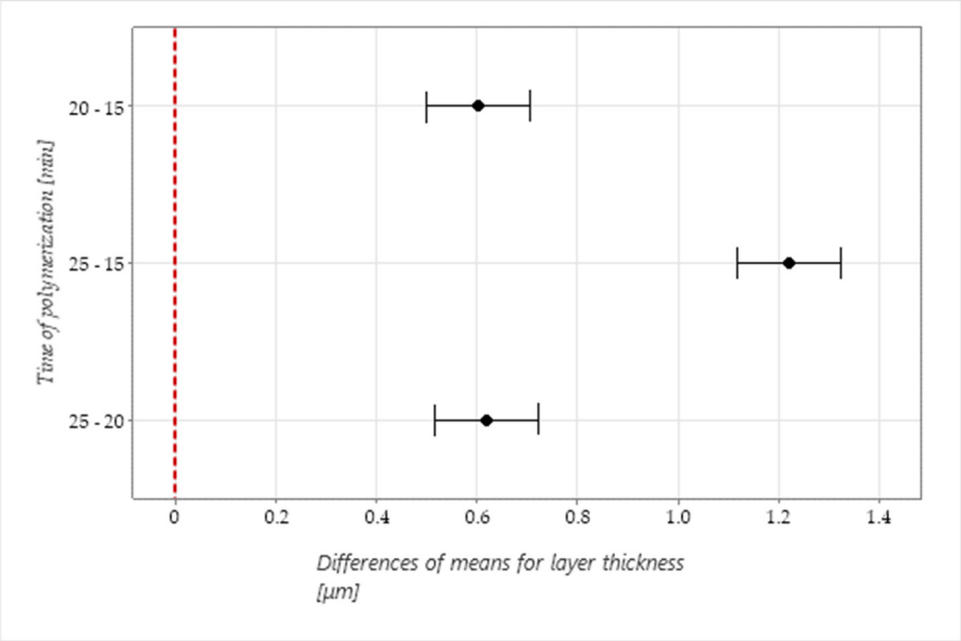

Figure 4. Values of differences in the thicknesses of the layer created by cataphoretic painting for uniform polymerization temperatures.

A graphic representation of the model verification (5) under the practical conditions of the production process is shown in Figure 5. The verification was carried out at U_{KTL} = 240 V on the same samples, listed in the Material Selection and Technological process of production section, and under the same conditions as the main experiment.

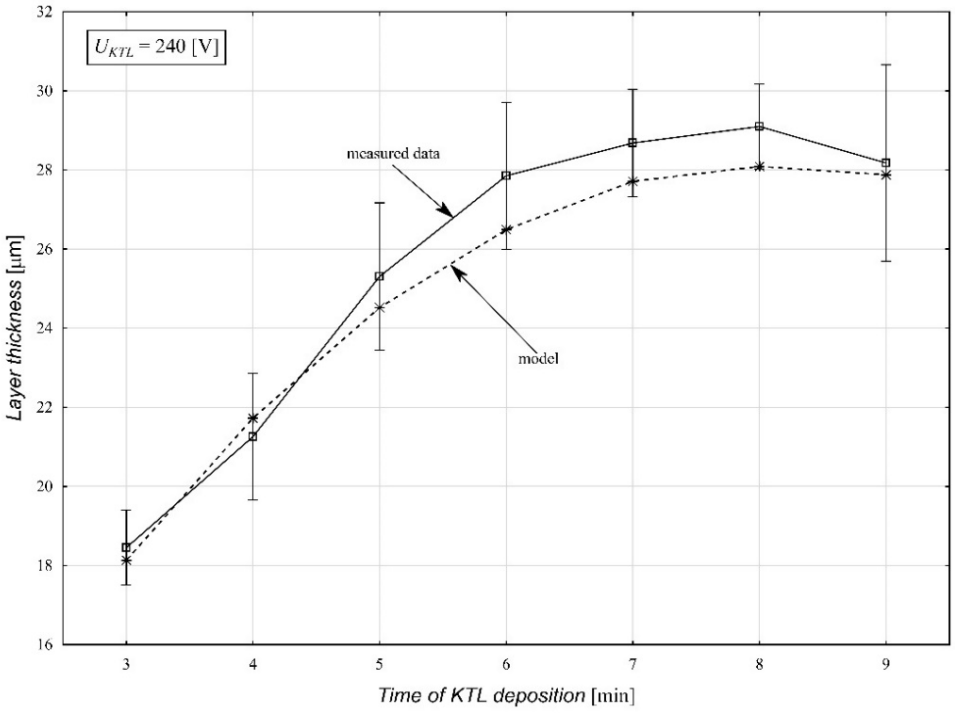

Figure 5. Graphical comparison of the thickness of the created layer within the verification experiment and the thickness of the layer calculated by the prediction model (5).

As part of the analysis of the modelled thickness values of the cataphoresis layer created and the values obtained from repeated measurements of the verification experiment, we came to conclusion that the average deviation in all the measurements carried out was 0.632 µm (2.14%), while the lowest negative deviation in the calculated thickness of the layer measured and the lowest deviation in the model (5) was at the level of −1.801 µm (8.690%), and the maximum positive value of the examined difference was at the level of +2.306 µm (8.407%). At the same time, based on the Shapiro–Wilks test, it can be said that the residues showed a normal Gaussian distribution (p = 0.233) at the selected level of significance, which indicated that the model (5) also met the last condition for the regression triplet analysis and could be considered correct. A graphical representation of the differences between the measured and modeled values of the thickness of the created layer is shown in Figure 6.

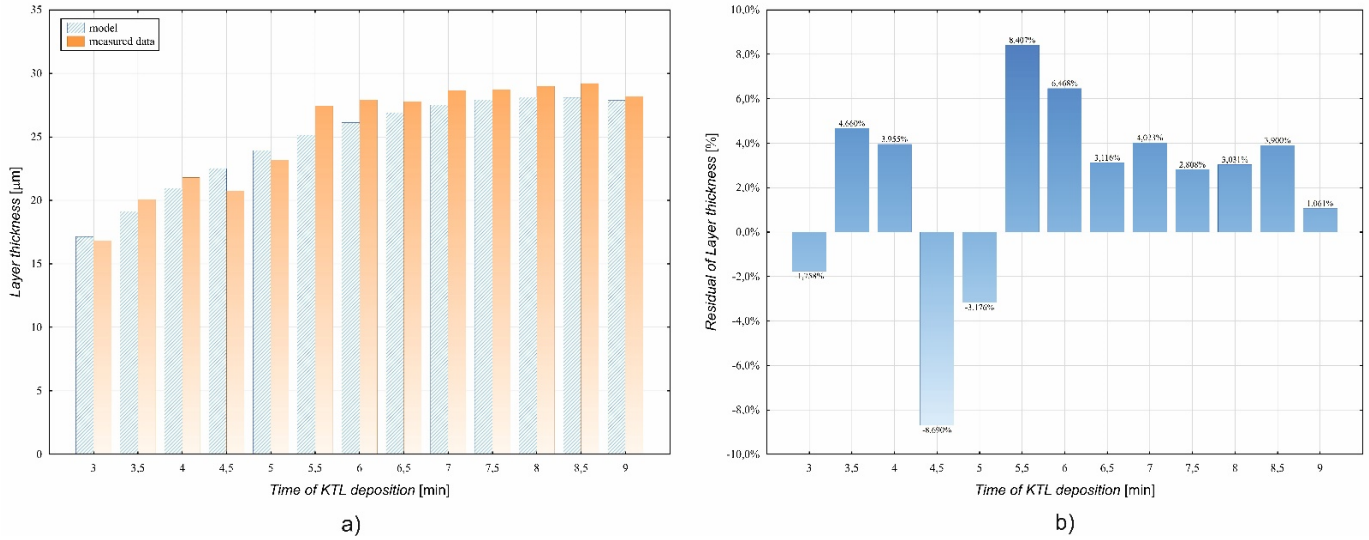

Figure 6. Differences between the measured and calculated thickness of the cataphoretic layer ((**a**) comparison of the results of the verification experiment and the model (5), and (**b**) percentage display of the residues for the verification experiment).

The morphology of the surface was also of significant importance from the point of view of the quality of the created cataphoretic layer. The change in the morphology and structure of the surface of the created layer depended primarily on the conditions of the process of creating the layer, that is, on the operation of the cataphoretic painting itself.

Figure 7 shows the surfaces of the layers created at voltages of U_{KTL} = 220 V, 260 V, and 280 V with deposition times of t_{KTL} = 7.5 min and 6.0 min at a constant polymerization temperature of 200 °C, but with a different polymerization times: 15 min (a), 20 min (b), and 25 min (c). It is clear from the mentioned morphologies that the tension in the process of creating the cataphoretic layer had a significant influence. At a voltage of 220 V, in all cases (a, b, c), a relatively smooth surface without a distinct structure was scanned. At a voltage of 260 V, morphological changes began to appear in the form of a slightly distinct structuring of the surface, but in the presence of a significant defect in the form of craters. These craters could be attributed to the process of cataphoretic painting in the form of the binding of the hydrogen on the surface of the painted sample with its binding by the created layer and subsequent "explosion" in the polymerization process. However, this defect was no longer observed when using a voltage of 280 V, but the surface of the created layer already had a pronounced wrinkled structure. In general, it can therefore be said that, by increasing the tension in the process of creating a layer, the morphology of the created layer deteriorated and the created layer acquired a significantly wrinkled structure.

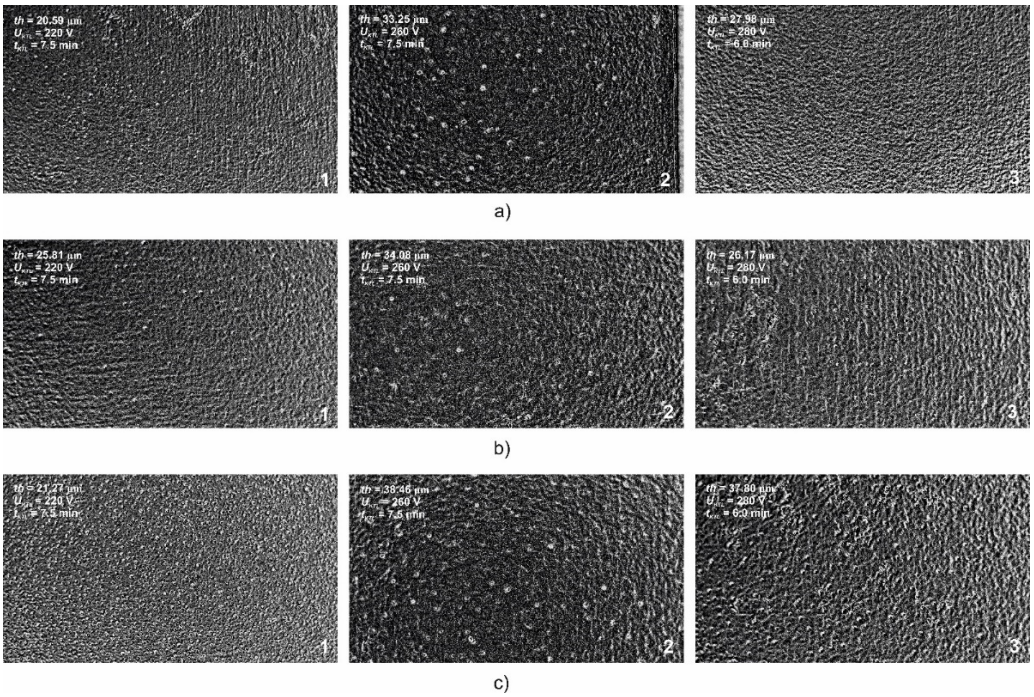

Figure 7. Morphological changes in the surface of the created cataphoretic layer depending on the voltage and the deposition time ((**a**) t_{POL} = 15 min, (**b**) t_{POL} = 20 min, and (**c**) t_{POL} = 25 min; 1—U_{KTL} = 220 V, t_{KTL} = 7.5 min, 2—U_{KTL} = 260 V, t_{KTL} = 7.5 min, and 3—U_{KTL} = 280 V, t_{KTL} = 6.0 min).

The confirmation of the above conclusions was carried out using additional experiments at a voltage of 400 V and deposition times of 5.0 min and 4.0 min, while the morphology of the surface of the cataphoretic layer is shown in Figure 8. It is obvious that the surface morphology of the formed layer at a high voltage was significantly structured with very pronounced wrinkling; however, with a deposition time of 5.0 min, the surface was significantly more heterogeneous than that in the case of a deposition time of 4.0 min. Thus, in addition to the applied voltage, the deposition time of the KTL process also had an effect on the surface morphology of the created cataphoretic layer and, with an increase in the deposition time, a more pronounced heterogeneity of the surface occurred.

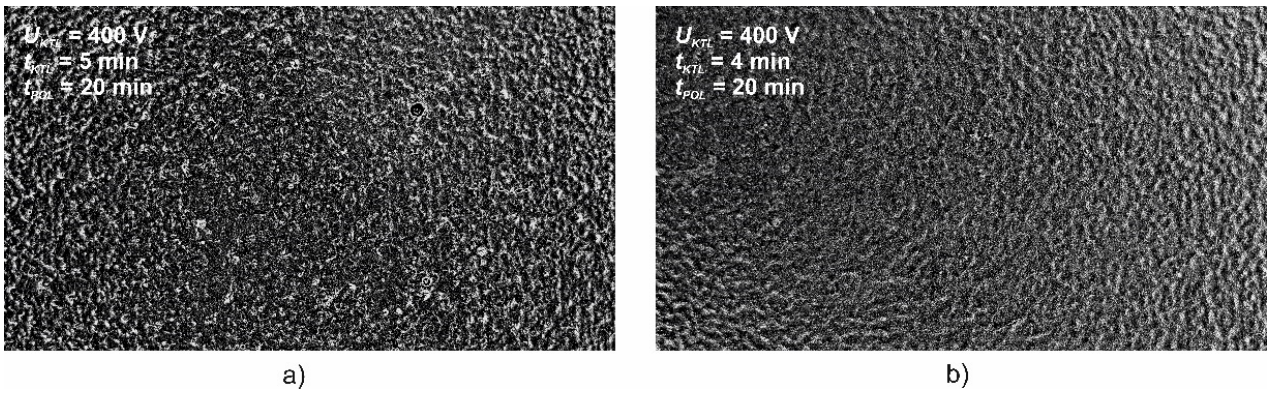

Figure 8. Morphological changes in the surface of the created cataphoresis layer at U_{KTL} = 400 V, t_{POL} = 20 min a T_{POL} = 200 °C ((**a**) t_{KTL} = 5 min, and (**b**) t_{KTL} = 4 min).

An important consequence of the defined predictive dependence (5) was a determination of the optimal values of the analyzed input variables (U, t_{KTL}). Due to the technological requirements placed on the thickness of the layer under formation, it was advisable to look for the maximum regression function (5). The general optimization problem was to select

n decision variables x_1; x_2; ... ; x_n from a given implemented area, in such a way as to optimize (minimize or maximize) the purpose function:

$$f(x_1, x_2, ..., x_n) \tag{8}$$

The optimization problem was a non-linear programming problem (*NLP*) if the purpose function was nonlinear or the implemented area was defined by nonlinear constraints. Then, the maximization of the general nonlinear programming is defined in the form of:

$$max f(x_1, x_2, ..., x_n) \tag{9}$$

for restrictions:

$$\begin{gathered} g_1(x_1, x_2, \ldots, x_n) \leq b_1 \\ g_2(x_1, x_2, \ldots, x_n) \leq b_2 \\ \ldots\ldots\ldots\ldots\ldots\ldots\ldots\ldots \\ g_m(x_1, x_2, \ldots, x_n) \leq b_m \end{gathered} \tag{10}$$

where each of the constraints g_1 through g_m is defined. A special case is linear programming. The obvious relation for this case is:

$$f(x_1, \ldots ..., x_n) = \sum_{j=1}^{n} c_j \cdot x_j \tag{11}$$

and

$$g_i(x_1, \ldots, ..., x_n) = \sum_{j=1}^{n} a_{ij} \cdot x_j i = (1, 2, ..., m) \tag{12}$$

Non-negative variables constraints can be included simply by attaching additional constraints:

$$g_{m+i}(x_1, x_2, ..., x_n) = -x_i \leq 0 i = (1, 2, ..., n) \tag{13}$$

In some cases, these constraints are considered explicit, as is any other issue in the delimited areas. In other cases, it is appropriate to consider them implicit if the non-negative constraints are manipulated, as is the case with simplex methods.

To simplify the proposition, let x denote the vector of the control variables x_1, x_2, ... , x_n, which represents x = (x_1, x_2, ... , x_n). The problem is more aptly written in the form:

$$max f(x) \tag{14}$$

according to the:

$$g_i(x) \leq b_i (i = 1, 2, .., m) \tag{15}$$

As in solving the tasks of linear programming, there are no restrictions on these formulations. When maximizing the $f(x)$ functions and, of course, also when minimizing its $f(x)$, the conditions of equality $h(x) = b$ can be written as two separate conditions of inequality, $h(x) \leq b$ and $-h(x) \leq -b$.

To optimize the thickness of the created cataphoresis layer, a regression model (5) was applied as a functional function and the interior point method was used for the nonlinear optimization. The ranges of the intervals of the variable input factors used were the basic constraints (Table 1), which are defined as follows:

$$200 \leq U \leq 2803 \leq t_{KTL} \leq 9 \tag{16}$$

A MATLAB software product Optimization Toolbox was used to implement the optimization of the thickness of the cataphoresis layer created. The task of the nonlinear optimization, in our case, was to find the maximum of the problem, which is defined as:

$$max f(x) \begin{cases} c(x) \leq 0 \\ ceq(x) = 0 \\ A \cdot x < b \\ Aeq \cdot x = beq \\ lb \leq x \leq ub \end{cases} \quad (17)$$

where x, b, beq, lb, and ub are vectors, A and Aeq are matrices, $c(x)$ and $ceq(x)$ are vector functions, and $f(x)$ is a scalar function. The course of the optimization process itself, as an output from the optimization program, is shown in Figure 9.

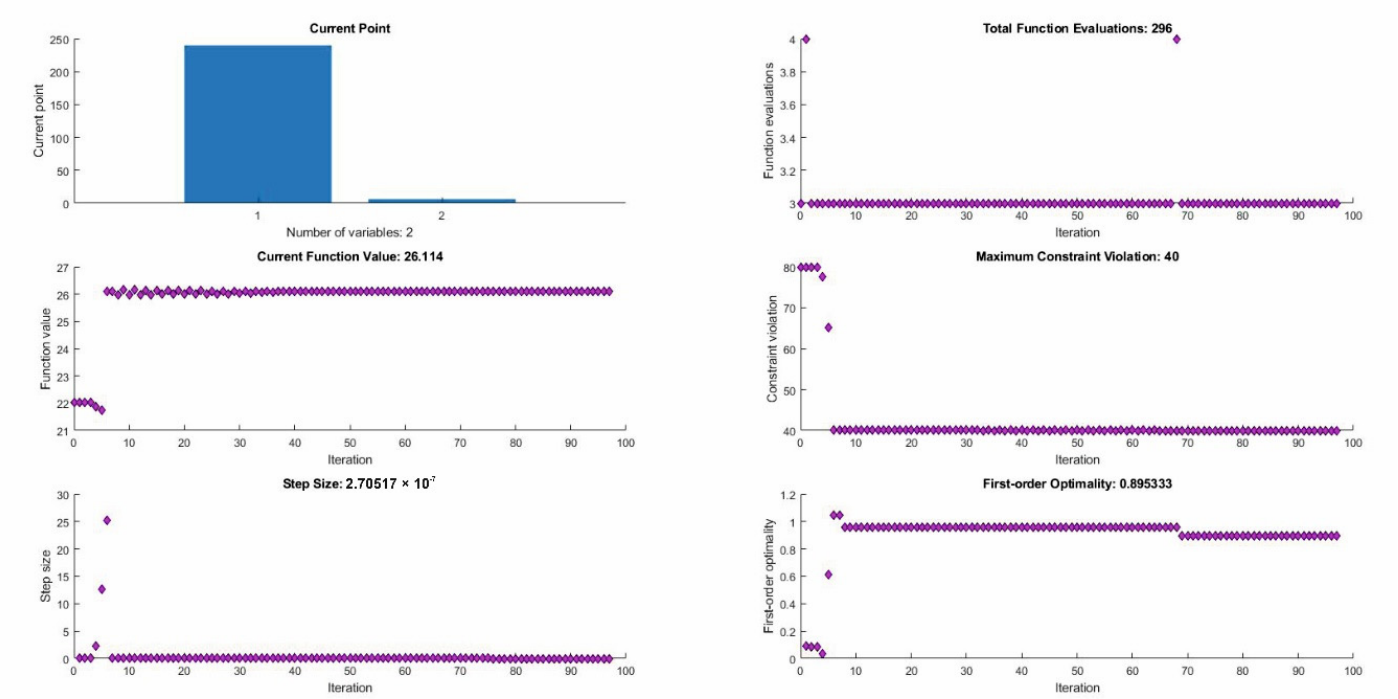

Figure 9. The course of optimization of the thickness of the created layer.

The result of the non-linear optimization process of the cataphoresis varnishing, considering only two variable technological factors, different voltages and deposition times in the process of the cataphoresis varnishing, was the determination of the maximum thickness of the purpose-built regression function (5). The maximum of the purpose-built function, while respecting the constraints given by Equation (16), was t_{hmax} = 26.114 µm under the following technological conditions: U = 240 V and t_{KTL} = 6.0 min. Therefore, in order to create the thickest layer possible, it was necessary to set these basic factors at a defined level [33].

However, we must also define the limitations of the conducted experimental research. The conclusions of the submitted study are valid only in the range of the experimental conditions listed in Table 1, which resulted from the applied statistical approach. A further limitation is imposed by the other relevant input conditions in the processes of degreasing, activation, and phosphating. Therefore, it will be necessary to expand the model (5) by including these impacts, thus defining the complex technological dependence of the process factors on the layer forming.

4. Conclusions

Today, cars are more than a means of transport for many, because they also create an image of the owner. Therefore, it is important what the vehicle looks like, which places demands not only on its design, but also on its surface treatment. Today's customers demand that its bodywork resists not only corrosion, which is achieved by using a good surface finish and high-quality varnishes, but also weather conditions (hail damage). Resistance to chemical influences that affect this bodywork, whether this is road salt or acid rain in winter, is also important. Progress in surface finishes and varnishing systems is constantly advancing. We can see this if we compare the technologies used 30 years ago to those used today. The treatment methods we use now are much more effective and environmentally friendly. This trend can also be observed in the surface treatment of bodywork, where, for example, the use of hexavalent chromium, which is toxic, is avoided. Great demands are placed on occupational safety, which is why quality and safe workplaces are essential. The varnishes and color shades used have also undergone a big transformation. The aim of the experimental part of this study was to create a planned experiment, on the basis of which, we analyzed the effects of varnishing voltage, varnishing current, deposition time, and layer thickness on the material surface. In total, 30 test samples of AW 1050—H24 were used. All the samples were passed through an automated cataphoresis varnishing line, from chemical degreasing to curing (polymerization). The thickness was then measured on the samples using a digital thickness gauge.

The initial analysis of the applied model pointed to the fact that the proportion of variability in the measured thickness of the cataphoresis coating was 86.70225% and the adjusted index of determination, determining the degree of explanation of data variability by the model, was 85.8775%. The average thickness of the layer formed in the process of cataphoresis, spanning all the individual trial runs, was $t_h = 24.464 \pm 3.677 \mu m$. Based on the analysis of variance, it can be said that the variability caused by random errors was significantly less than the variability in the measured values. Based on the model of significance achieved, this indicated that this model is suitable for use. Under the voltage of 220 V, the thickness of the coating increased for 5.5 min, when the coating also reached its maximum thickness. After this time, the thickness of the coating decreased. Increasing the varnishing voltage to 240 V meant increasing the deposition time of the varnishing medium up to 8 min, without significantly affecting the thickness of the layer. A further increase in the varnishing voltage resulted in an accelerated layer formation, and a similar change was observed when the varnishing voltage was increased to 260 V and 280 V, when the thickness of the layer reached its maximum values throughout the deposition time of the varnishing medium t in the electrolyte.

The authors see the submitted paper as a contribution to the procedural approach to such complex processes of creating anti-corrosion layers, such as the process of cataphoresis varnishing. Since the surface treatment technological processes represent multifactor systems with interacting physical, chemical, and technological effects and, at the same time, since the influences may be considered as random variables, the authors subjected the experimentally obtained data to the correct methods of statistical analysis for a deeper understanding of these interrelationships. Another undisputed benefit of the present paper is the nonlinear optimization (maximization) of the basic technological parameter, the thickness of the created layer, and the analysis of the rate of the cataphoresis coating deposition. However, its limitations are those of the experiment constraints and the use of only two basic process factors.

However, it should be remembered that the process of creating a cataphoresis layer is a complex physical and chemical process, where the formation of bonds between the individual components of the cataphoresis paint, under the influence of an electric current, plays an essential role. Although mathematical models for the formation and growth of the cataphoresis layer [2] describe the causes of and, at the same time, the inter-relations between the factors involved in the growth of the cataphoresis layer, in relatively great detail, the authors' effort was to simplify the prediction of the thickness of the layer based on

the practically used input factors in the KTL process, namely, the change in the deposition time and stress in the cataphoresis coating. Another fact is that the resulting property, the quality of the layer formed by cataphoresis, is not determined only by its thickness. The quality of the cataphoresis layer is also the result of its other properties, such as corrosion resistance, adhesion, bending, impact resistance, and hardness, as well as its aesthetic properties expressed by gloss and shade. All of these properties can be influenced within the complex KTL process, starting with pre-treatment and ending with polymerization. However, as part of the present paper, we focused only on the analysis of the thickness of the created cataphoresis layer as a basic parameter, which is prescribed in a customer's drawing documentation as a requirement for the painting process, which also affects the other, above-mentioned properties of the layer to some extent.

Author Contributions: Conceptualization, J.D. and M.G.; methodology, M.G.; validation, P.F.; formal analysis, R.B.B.; data curation, P.F. and R.B.B.; writing original draft preparation, J.D. All authors have read and agreed to the published version of the manuscript.

Funding: This research received no external funding.

Institutional Review Board Statement: Not applicable.

Informed Consent Statement: Not applicable.

Data Availability Statement: Not applicable.

Acknowledgments: This paper has been elaborated in the framework of the project KEGA 063TUKE-4/2021.

Conflicts of Interest: The authors declare no conflict of interest. The founding sponsors had no role in the design of the study; in the collection, analyses, or interpretation of the data; in the writing of the manuscript; or in the decision to publish the results.

References

1. Brüggemann, M.; Rach, A. *Electrocoat*; Vincentz Verlag: Hannover, Germany, 2020.
2. Goldschmidt, A.; Streitberger, H.J. *BASF-Handbuch: Lackiertechnik*; Vincentz Verlag: Hannover, Germany, 2002.
3. Brock, T.; Groteklaes, M.; Mischke, P. *European Coatings Handbook*, 2nd ed.; Vincentz Verlag: Hannover, Germany, 2010.
4. Akafuah, N.K.; Poozesh, S.; Salaimeh, A.; Patrick, G.; Lawler, K.; Saito, K. Evolution of the Automotive Body Coating Process-A Review. *Coatings* **2016**, *6*, 24. [CrossRef]
5. Skotnicki, W.; Jedrzejczyk, D. The comparative analysis of the coatings deposited on the automotive parts by the cataphoresis method. *Materials* **2021**, *14*, 6155. [CrossRef] [PubMed]
6. Mazeran, P.E.; Arvieu, M.F.; Bigerelle, M.; Delalande, S. Torsion delamination test, a new method to quantify the adhesion of coating: Application to car coatings. *Prog. Org. Coat.* **2017**, *110*, 134–139. [CrossRef]
7. Romano, A.P.; Olivier, M.G.; Vandermiers, C.; Poelman, M. Influence of the curing temperature of a cataphoretic coating on the development of filiform corrosion of aluminium. *Prog. Org. Coat.* **2006**, *57*, 400–407. [CrossRef]
8. Miskovic-Stankovic, V.B.; Stanic, M.R.; Drazic, D.M. Corrosion protection of aluminium by a cataphoretic epoxy coating. *Prog. Org. Coat.* **1999**, *36*, 53–63. [CrossRef]
9. Olivier, M.G.; Poelman, M.; Demuynck, M.; Petitjean, J.P. EIS evaluation of the filiform corrosion of aluminium coated by a cataphoretic paint. *Prog. Org. Coat.* **2005**, *52*, 263–270. [CrossRef]
10. Rossi, S.; Calovi, M.; Fedel, M. Corrosion protection of aluminum foams by cataphoretic deposition of organic coatings. *Prog. Org. Coat.* **2017**, *109*, 144–151. [CrossRef]
11. Poulain, V.; Petitjean, J.P.; Dumont, E.; Dugnoille, B. Pretreatments and filiform corrosion resistance of cataphoretic painted aluminium characterization by EIS and spectroscopic ellipsometry. *Electrochim. Acta* **1996**, *41*, 1223–1231. [CrossRef]
12. Almeida, E.; Alves, I.; Brites, C.; Fedrizzi, L. Cataphoretic and autophoretic automotive primers: A comparative study. *Prog. Org. Coat.* **2003**, *46*, 8–20. [CrossRef]
13. Deflorian, F.; Rossi, S.; Prosseda, S. Improvement of corrosion protection system for aluminium body bus used in public transportation. *Mater. Des.* **2006**, *27*, 758–769. [CrossRef]
14. Su, Y.; Zhitomirsky, I. Cataphoretic assembly of cationic dyes and deposition of carbon nanotube and graphene films. *J. Colloid Interface Sci.* **2013**, *399*, 46–53. [CrossRef] [PubMed]
15. Rudawska, A.; Wahab, M.A. The effect of cataphoretic and powder coatings on the strength and failure modes of EN AW-5754 aluminium alloy adhesive joints. *Int. J. Adhes. Adhes.* **2019**, *89*, 40–50. [CrossRef]
16. Calovi, M.; Dire, S.; Ceccato, R.; Deflorian, F.; Rossi, S. Corrosion protection properties of functionalised graphene–acrylate coatings produced via cataphoretic deposition. *Prog. Org. Coat.* **2019**, *136*, 105261. [CrossRef]

17. Rossi, S.; Calovi, M. Addition of graphene oxide plates in cataphoretic deposited organic coatings. *Prog. Org. Coat.* **2018**, *125*, 40–47. [CrossRef]
18. Zanella, C.; Fedel, M.; Deflorian, F. Correlation between electrophoretic clearcoats properties and electrochemical character-istics of noble substrates. *Prog. Org. Coat.* **2012**, *74*, 349–355. [CrossRef]
19. Fedel, M.; Druart, M.E.; Olivier, M.; Poelman, M.; Deflorian, F.; Rossi, S. Compatibility between cataphoretic electro-coating and silane surface layer for the corrosion protection of galvanized steel. *Prog. Org. Coat.* **2010**, *69*, 118–125. [CrossRef]
20. Romano, A.P.; Fedel, M.; Deflorian, F.; Olivier, M.G. Silane sol-gel film as pretreatment for improvement of barrier properties and filiform corrosion resistance of 6016 aluminium alloy covered by cataphoretic coating. *Prog. Org. Coat.* **2011**, *72*, 695–702. [CrossRef]
21. Manas, D.; Manas, M.; Gajzlerova, L.; Ovsik, M.; Kratky, P.; Senkerik, V.; Skrobak, A.; Danek, M.; Manas, M. Effect of low doses beta irradiation on micromechanical properties of surface layer of injection molded polypropylene composite. *Radiat. Phys. Chem.* **2015**, *114*, 25–30. [CrossRef]
22. Mishra, R.; Behera, B.K.; Muller, M.; Petru, M. Finite element modeling based thermodynamic simulation of aerogel embedded nonwoven thermal insulation material. *Int. J. Therm. Sci.* **2021**, *164*, 106898. [CrossRef]
23. Botko, F.; Hatala, M.; Beraxa, P.; Duplak, J.; Zajac, J. Determination of CVD Coating Thickness for Shaped Surface Tool. *TEM J. Technol. Educ. Manag. Inform.* **2018**, *7*, 428–432. [CrossRef]
24. Jurko, J.; Panda, A.; Gajdos, M.; Zaborowski, T. Verification of Cutting Zone Machinability during the Turning of a New Austenitic Stainless Steel. *Adv. Comput. Sci. Educ. Appl.* **2011**, *202*, 338.
25. Behalek, L.; Novak, J.; Brdlik, P.; Boruvka, M.; Habr, J.; Lenfeld, P. Physical Properties and Non-Isothermal Crystallisation Kinetics of Primary Mechanically Recycled Poly(l-lactic acid) and Poly(3-hydroxybutyrate-co-3-hydroxyvalerate). *Polymers* **2021**, *13*, 3396. [CrossRef] [PubMed]
26. Svetlik, J.; Malega, P.; Rudy, V.; Rusnak, J.; Kovac, J. Application of Innovative Methods of Predictive Control in Projects Involving Intelligent Steel Processing Production Systems. *Materials* **2021**, *14*, 1641. [CrossRef] [PubMed]
27. Milosevic, M.; Cep, R.; Cepova, L.; Lukic, D.; Antic, A.; Djurdjev, M. A Hybrid Grey Wolf Optimizer for Process Planning Optimization with Precedence Constraints. *Materials* **2021**, *14*, 7360. [CrossRef] [PubMed]
28. Nova, I.; Frana, K.; Solfronk, P.; Sobotka, J.; Korecek, D.; Svec, M. Characteristics of Porous Aluminium Materials Produced by Pressing Sodium Chloride into Their Melts. *Materials* **2021**, *14*, 4809. [CrossRef]
29. Baron, P.; Kocisko, M.; Blasko, L.; Szentivanyi, P. Verification of the operating condition of stationary industrial gearbox through analysis of dynamic signal, measured on the pinion bearing housing. *Measurement* **2017**, *96*, 24–33. [CrossRef]
30. Panda, A.; Duplak, J.; Jurko, J.; Behun, M. New experimental expression of durability dependence for ceramic cutting tool. *Appl. Mech. Mater.* **2013**, *275–277*, 2230–2236. [CrossRef]
31. Cuha, D.; Hatala, M. Effect of a modified impact angle of an ultrasonically generated pulsating water jet on aluminum alloy erosion using upward and downward stair trajectory. *Wear* **2022**, *500*, 204369. [CrossRef]
32. Bukovska, S.; Moravec, J.; Solfronk, P.; Pekarek, M. Assessment of the Effect of Residual Stresses Arising in the HAZ of Welds on the Fatigue Life of S700MC Steel. *Metals* **2022**, *12*, 1890. [CrossRef]
33. Kamble, Z.; Mishra, R.K.; Behera, B.K.; Tichy, M.; Kolar, V.; Muller, M. Design, Development, and Characterization of Advanced Textile Structural Hollow Composites. *Polymers* **2021**, *13*, 3535. [CrossRef]